SSRG International Journal of Mechanical Engineering
ISSN: 2348-8360/ https://doi.org/10.14445/23488360/IJME-V12I2P108

Volume 12 Issue 2, 88-106, February 2025
© 2025 Seventh Sense Research Group®

Original Article

Investigation of Sequential Port Fuel Injection over Manifold Fuel Injection to Evaluate Combustion and Emission Parameters in Spark Ignition Engine Using Hydrogen Enriched CNG Blends

Pravin Nitnaware[1], Vishal Meshram[2], Ravikant Nanwatkar[3], Amit R. Patil[4]

[1]*Department of Mechanical Engineering, D. Y. Patil College of Engineering, SPPU, Pune, Maharashtra, India.*
[2]*Department of Mechanical Engineering, Indira College of Engineering and Technology, SPPU, Pune, Maharashtra, India.*
[3]*Department of Mechanical Engineering, Sinhgad College of Engineering, SPPU, Pune, Maharashtra, India.*
[4]*Department of Mechanical Engineering, MES Wadia College of Engineering, SPPU, Pune, Maharashtra, India.*

[3]*Corresponding Author : ravikant.nanwatkar@sinhgad.edu*

Received: 13 December 2024 Revised: 11 January 2025 Accepted: 12 February 2025 Published: 25 February 2025

Abstract - *The demand for clean and eco-friendly fuels has driven extensive research on hydrogen blended natural gas in Spark Ignition (SI) Engines. This study investigates the performance, emissions and combustion characteristics of a 10 % Hydrogen blend in a 3-cylinder SI engine utilizing both Sequential-Port-Fuel-Injection (SPFI) and Conventional-Manifold -Fuel- Injection (CMFI) systems. Experiments were conducted at Wide Open Throttle (WOT) and Minimum advance for Best Torque (MBT) Spark Timing across engine speeds of 2000-4000 rpm under varying loads using an eddy-current dynamometer. The results indicate that SPFI enhances power output, Brake Thermal Efficiency (BTE) and combustion characteristics while reducing Hydrocarbon (HC) and Carbon Monoxide (CO) emissions. However, it also leads to increased Nitrogen Oxides (Nox) emissions. In contrast, CMFI exhibited higher Break-Specific Fuel Consumption (BSFC) and lower Nox emissions due to reduced volumetric efficiency and natural aspiration constraints, leading to a decrease in power and efficiency. Key combustion parameters, including in-cylinder pressure, Rate of Pressure Rise and Net Heat Release Rate, were also analyzed. The study provides valuable insights into the impact of injection strategies on HCNG combustion, offering potential pathways for optimizing fuel delivery systems in SI engines for improved efficiency and emission control.*

Keywords - *HCNG Blends, SPFI, CMFI, Nox, NHRR, Pmax.*

1. Introduction

The role of the fuel injection system is crucial for improving both emissions and performance in SI engines. In Spark Ignition (SI) engines, Sequential Port Fuel Injection (SPFI) and Conventional Manifold Fuel Injection (CMFI) systems are utilized. SPFI is preferred because it precisely controls fuel delivery. A separate injector, located near the inlet port, injects fuel at a specified pressure as per the engine load and speed. By improving the mass flow of the air-fuel mixture, SPFI increases the engine's power output and enhances charge intake. Sensors such as the Oxygen (O_2) sensor, Throttle Position Sensor (TPS), Manifold Absolute Pressure (MAP) sensor, and exhaust temperature sensor provide data to the injector system. This information is mapped to the Engine Control Unit (ECU), allowing precise fuel injection for each engine stroke. This precise control lowers exhaust emissions while improving performance standards. For SI engines, Gasoline Direct Injection (GDI) is also used, but it requires highly accurate injectors to maintain high cylinder pressures and temperatures under load conditions. Since there is very little time for the fuel to vaporize, GDI injects fuel at very high pressure; otherwise, it is going to increase harmful emissions, i.e. Particulate Matter (PM) and hard carbon. Lean-burn combustion is easily achieved with both GDI and SPFI systems. Specially designed high-pressure injectors are necessary for the GDI system to accommodate the high diffusivity of hydrogen. The most effective way to improve CNG combustion is through hydrogen addition, which facilitates lean-burn combustion and increases flame speed. Blending 10% hydrogen by volume with CNG has been found to be optimal for enhancing combustion. The high-octane number of CNG, combined with the high calorific value of hydrogen, as well as their broader flammability limits and greater diffusivity, contribute to raising the mixture's flame speed. This results in increased

This is an open access article under the CC BY-NC-ND license (http://creativecommons.org/licenses/by-nc-nd/4.0/)

combustion efficiency and cleaner exhaust emissions. In CMFI, HC emissions are higher in exhaust due to the non-uniform distribution of charge in each cylinder. The flow rate of charge is adjusted manually and remains constant during all speeds. Due to the low volumetric efficiency of naturally aspirated SI engines, Power output is reduced. In CMFI, there are more chances of backfiring during valve overlap in an SI engine. In SPFI, the fuel supply is controlled by a sensor. Uniform distribution of charge to each cylinder is done by a separate injector near the inlet port. NOx emissions are more at a higher speed due to complete combustion. More power output is observed at a higher speed compared to conventional fuel injection systems. SPFI gives higher fuel economy due to complete combustion. Emissions are reduced due to complete combustion.

Table 1. Comparison of properties of hydrogen methane and gasoline

Property	Units	Hydrogen	Methane
Auto-ignition temp.	K	858	813
Stoichiometric air composition	% by volume	29.53	9.48
Combustion energy per kg of stoichio. mixture	mJ	3.37	2.56
Density (gas) at 1 atmp. and 300 K	kg/m^3	0.082	0.717
Density (liquid)	kg/lit	0.071	0.42
Diffusion coeff. in air at NTP	cm^2/s	0.61	0.189
Equivalence ratio, ignition lower limit in NTP air	--	0.10 - 7.1	0.7 - 4
Energy of stoichiometric mixture	mJ/m^3	3.6	3.5
Flame temp. in air at λ=1 (adiabatic)	K	2318	2190
Higher Heating Value	MJ/kg	141.7	52.68
Higher Heating Value	MJ/m^3	12.10	37.71
Kinematic viscosity at 300 K	mm^2/s	110	17.2
Laminar burning velocity at NTP	m/s	3.25	0.38
Lower Heating Value	MJ/kg	120	46.72
Lower Heating Value	MJ/m^3	10.22	33.95
Minimum energy for ignition in air	mJ	0.02	0.29
Molar Carbon to Hydrogen ratio	--	0	0.25
Normal boiling point	K	20.3	111.6
Quenching the gap at NTP	mm	0.64	2.03
Octane Number	--	130+	125
Stoichiometric Fuel/Air mass	--	0.029	0.058
Thermal conductivity at 300K	mW/m.K	182.0	34.0
Thermal energy radiated from the flame to the surrounding	%	17-25	23-33
Volumetric LHV at NTP	kJ/m^3	10046	32573
Volumetric fraction of fuel in air Ø=1 at NTP	--	0.290	0.095
Specific mixture energy	kJ/m^3		3200
CO_2 formation	$gm.CO_2/kWh$	Nil	200
Tank volume (equal to gasoline)	litre		200
Flammability limits	% by volume	4 - 75	5.3 - 15.0

Table 2. HCNG properties

Properties	CH4	5 vol %	10 vol %	15 vol %
Volumetric Fraction H_2 (vol %)	0	5	10	15
Volumetric Fraction CH_4 (vol %)	100	95	90	85
Mass Fraction H_2 (vol %)	0	0.705	1.377	2.169
Mass Fraction CH_4 (vol %)	100	99.29	98.623	97.831
Energy substitution H_2 (%)	0	1.652	3..242	5.053
Stoichiometric Air Ratio	17.19	17.23	17.26	17.284
Low Heating Value (MJ/kg)	50.02	50.492	50.964	51.519
Mass Fraction of H (Mass %)	25.13	25.62	26.16	26.75
Mass Fraction of C(Mass %)	74.87	74.38	73.84	73.25
Lower Heating value (MJ/m^3)	3.170	3.167	3.164	3.160

P-Ɵ diagram shows an increase in peak pressure compared to a conventional fuel supply system. Lambda sensors control the fuel supply during all speeds and protect against loss of excess fuel during different load conditions. A spark advancer is used in CNG to increase the spark advance with an increase in speed for maximum brake torque.

Table 3. HCNG blend properties: at 98 kpa, 300 k

Sr No	Property	Units	CNG	10 HCNG	20 HCNG	30 HCNG	40 HCNG	50 HCNG
1	Density	Kg/m^3	0.5196	0.5931	0.5362	0.4793	0.42248	0.3656
2	Mass Fraction of hydrogen	%	0	1.369	3.0303	5.084	7.6923	11.11
3	Mass Fraction of CH4	%	100	98.63	96.96	94.91	92.30	88.88
4	Mass Fraction of H	%	25	32.98	27.27	28.813	30.77	33.33
5	Mass Fraction of C	%	75	73.97	72.72	71.186	69.23	66.66
6	Lower Heating Value	kJ/kg	50,000	50954	52084	53556	55380	57772
7	Lower Heating Value	Kcal/kg	11945	12173	12443	12794		13801
8	Lower Heating Value	kJ/m^3	32495	30224	27927	25669		21121
9	C/H ratio		0.25	0.2368	0.2222	0.2058	0.1875	0.1666
10	Energy Substitution	%	-	2.223	6.9119	11.382	16.66	23.07
11	Stoichiometric A: F Ratio		17.16	17.39	17.68	18.039	18.487	19.07

The chances of brake fire are reduced due to the fuel injector present near each inlet port and only open during suction stroke. Unburnt fuel is reduced in exhaust due to complete combustion. HC and CO emissions are reduced due to the desired fuel injection in the cylinder. Flame trap and flame arrester reduce chances of backfire/blast in exhaust line during running at higher speed. MFB and Heat release rate increases with sequential injection due to complete combustion. Peak pressure increases due to precise fuel control maintained in sequential injection.

1.1. Problem Statement

The need to substitute cleaner and more energetic alternatives thus evokes a lot of attention to the use of Hydrogen-enriched Compressed Natural Gas (HCNG) blends for the effective reduction of greenhouse gases and exhaust emissions in internal combustion engines. HCNG blends provide environmental and performance benefits, but their effectiveness relies strongly on the fuel injection strategy used. However, multicylinder SI engines with CMFI systems usually suffer from complex issues such as less than optimal mixing of fuel-air, emission increments, and less than optimal distribution among cylinders. Sequential Port Fuel Injection (SPFI) systems, on the other hand, can eliminate these drawbacks with accurately timed injection and improved atomization. Still, the relative advantages of SPFI vs. CMFI in the context of 10.

1.2. Objectives

1.2.1. Evaluate Performance Metrics

The comparison of BTE, BSFC, and Torque for SPFI & CMFI systems based on 10%HCNG blends in MPFI Multicylinder SI engines

1.2.2. Analyze the Combustion Properties

Evaluate combustion characteristics such as in-cylinder pressure, pressure rise rate, heat release rate, and combustion stability to elucidate the impact of SPFI and CMFI on combustion performance and stability.

1.2.3. Assess Emission Profiles

Quantify and compare emissions such as NOx, CO, HC, and PM emissions to model the environmental impact of SPFI and CMFI systems with HCNG blends.

1.2.4. Optimize Fuel-Air Mixing

Study the air-fuel mixing in SPFI and CMFI systems to see their effect on uniformity in Multicylinder configurations, which affect combustion efficiency.

1.2.5. Recognize Trade-offs and Challenges

Discuss the challenges like NOx formation with HCNG blends and trade-offs for different injection systems that will contribute understanding to their practical implementations.

1.2.6. Provide Recommendations

Provide suggestions to improve performance and emissions with HCNG blends in MPFI Multicylinder SI engines by optimizing the SPFI timing and the CMFI parameters types.

1.2.7. Pitch in with Eco-Friendly Solutions

Emphasize the promising potential of HCNG blends in reducing carbon-based emissions and developing high-potential sustainable fuel sources in automotive applications.

2. Literature Survey

An experimental study on a port injection engine using 10%, 30%, and 50% isobutanol-gasoline blends demonstrated that iso-butanol is a promising drop-in fuel for SI engines. It can be blended in higher concentrations than ethanol without requiring modifications to the fuel system or engine components [1]. Compressed Natural Gas (CNG) is a leading

alternative to fossil fuels due to its global availability, cleaner combustion, cost-effectiveness, and compatibility with gasoline and diesel engines. Key areas of focus include CNG vehicle economics, engine design and recital, ignition and fuel inoculation features, CNG/diesel double-fuel processes, hydrogen-augmented CNG schemes, conservational assistances, and safety considerations [2]. Multipoint injection systems in HCCI engines require precise control of mixture composition for optimal auto-ignition timing, with the most effective injection occurring when the intake valve is open.

During cold starts, fuel spray interacts with airflow and surfaces, potentially forming liquid films and generating smaller droplets through secondary atomization. Experiments under controlled conditions show that cross-flow decelerates droplet velocity, reducing impact energy and resulting in thinner films. This promotes the generation of secondary droplets, which are carried away, preventing re-impact on surfaces. The findings aid in the development of spray/wall interaction models [3]. A chassis dynamometer study compared particle emissions from a Port Fuel Injection (PFI) and a Gasoline Direct Injection (GDI) vehicle, focusing on particle number, surface area, volume, and size distributions (30 nm to 1 μm). Under the NEDC, the GDI vehicle's emissions were significantly higher than the PFI's, with particle number, surface area, and volume emissions being 5.3, 9.0, and 14.6 times greater, respectively. The GDI vehicle also exhibited larger particle sizes.

In the Full-load Steady-state Condition (FSE), the GDI vehicle's emissions were up to 39.8 times higher than the PFI's [4]. Ethanol is a renewable alternative fuel for internal combustion engines, and Ethanol Direct Injection plus Gasoline Port Injection (EDI + GPI) systems have been studied to optimize its use. Ethanol's high latent heat, fast flame speed, and wide flammability enhance anti-knock ability and lean burn performance. Experiments on a 250 cc SI engine investigated the effects of ethanol Start of Injection (SOI) timing. Late Injection (LEDI) effectively reduced knock but lowered efficiency and raised emissions.

Early Injection (EEDI) improved volumetric efficiency, extended the lean burn limit, and increased engine thermal efficiency while reducing emissions [5]. A study on a common rail diesel engine transformed to double-fuel mode investigated the effects of natural gas injection timing on combustion and emissions at low load under varying pilot injection pressure and timing. Results showed that retarding natural gas injection timing improved combustion performance and emissions by creating a stratified air-fuel mixture. Higher pilot injection pressure (72 MPa) improved combustion efficiency but increased emissions. Advanced pilot injection timing (17 ATDC) enhanced combustion, reducing THC and CO emissions but raising NOx levels. Optimizing natural gas inoculation effectiveness through experimental constraints is key to improving dual-fuel engine performance at low loads [6]. Ethanol Direct Injection combined with Gasoline Port Injection (EDI + GPI) improves ethanol utilization in spark ignition engines. A Computational Fluid Dynamics (CFD) study modelled in-cylinder flow, spray breakup, and combustion for EDI + GPI under single and dual-fuel conditions.

The results showed that EDI + GPI operates in a partially premixed combustion mode due to ethanol's low evaporation rate in low-temperature environments. Compared to gasoline port injection alone, EDI + GPI achieved higher power output and thermal efficiency, with reduced NOx emissions due to ethanol's lower adiabatic flame temperature and cooling effect.

However, CO and HC emissions increased due to incomplete combustion from ethanol's slow evaporation [7]. The energy catastrophe and conservational anxieties highlight the appeal of substitute fuels for reducing fuel consumption and emissions. Ethanol, with its high octane number, improved anti-knock characteristics, and higher heat of vaporization, enhances engine efficiency and power output while reducing emissions. Methane, with better anti-knock properties and lower CO_2 emissions, is another promising fuel but has slower flame propagation and lower power output. Adding hydrogen improves combustion and extends lean operation.

This study analyzed the effects of gasoline, ethanol, methane, and hydrogen-methane blends on engine performance using optical techniques to monitor combustion and measure emissions [8]. The study examined the effects of methanol-ultralow sulfur gasoline blends (0%, 15%, and 45% methanol by capacity) on an automatically measured multipoint port inoculation engine. Using a DMS 500SKII spectrometer, particulate mass, number concentrations, and size distributions were measured. Outcomes displayed that methanol increased cylinder compression and heat issue proportion, particularly at higher engine loads. Low methanol blends reduced particulate emissions, while high methanol blends increased them.

Particle number concentrations in the nucleation mode rose with engine load, while accumulation mode particles decreased at higher loads [9]. The study investigated the ignition and emissions of a Twin Fuel Consecutive Ignition (TFSC) style by port fuel inoculated n-heptane through in-cylinder straight inoculation of ethanol, n-butanol, and n-amyl alcohol in a sole-cylinder engine. Heat issues arise in phases of short and high-temperature response of n-heptane, along with direct fuel combustion. The amount of n-heptane affects peak in-cylinder pressure and temperature. Higher premixed ratios reduce CO emissions at high Lower Heating Values (LHVs) while increasing CO at medium and low LHVs. NOx and soot emissions remained low, with ethanol producing the lowest levels due to its higher latent heat and lower cetane

number. Optimized n-butanol injection at low loads achieved thermal efficiency of over 46% with low emissions [10]. Ethanol Direct Injection plus Gasoline Port Injection (EDI + GPI) enhances ethanol use in spark ignition engines but faces challenges with ethanol's low vapor pressure and high latent heat, which slow evaporation and increase CO and HC emissions.

Heating the ethanol fuel (EDI heating) was proposed to address this. The study found that EDI heating significantly reduced CO and HC emissions, especially at higher ethanol ratios, by improving evaporation and reducing fuel impingement. While NOx emissions slightly increased, they remained lower than in GPI-only conditions. EDI heating slightly reduced IMEP due to flash-boiling but allowed improvements in engine performance when spark timing was optimized, making it an effective solution for EDI + GPI engines [11]. The study scrutinizes the properties of fuel inoculation approaches and ambient temperature on automobile releases after Gasoline Direct Injection (GDI) and Port Fuel Injection (PFI) vehicles by conformist and ethanol-blended gasoline (E10). Testing at 7°C and 30°C revealed that lower temperatures significantly increased fuel consumption and emissions (except NOx). While the GDI vehicle had better fuel efficiency, it emitted more Total Hydrocarbons (THC), Particulate Matter (PM), and solid Particle Numbers (PN) at 30°C. In cold conditions, the PFI vehicle showed higher CO, THC, and PM emissions, with particulate emissions during start-up significantly higher than GDI. The results highlight the need to consider PFI emissions in cold environments [12].

The study investigates the jet characteristics of high-pressure hydrogen injection in a constant volume chamber, focusing on its effects on mixture formation and backfire prevention in hydrogen internal combustion engines. Results show that hydrogen penetration rate increases with higher injection pressure and decreases with rising ambient pressure. Injection pulse width had no significant impact. When the ratio of injection to ambient pressure exceeds 2.5, the hydrogen injection forms a continuous column. A 3D model for port Fuel Injection (PFI) hydrogen engines was developed, and experimental results validated the CFD model under various conditions, helping to optimize injection strategies to meet power demands while avoiding backfire [13]. Gasoline Direct Injection (GDI) engines, widely adopted to reduce fuel consumption, emit significantly more solid particles (PN) and Black Carbon (BC) compared to Multi-Port Fuel Injection (MPFI) engines. A study measuring emissions from four GDI and four MPFI vehicles revealed that GDI vehicles, particularly those deprived of particle filters, produce higher PN and BC emissions, especially under cold-start and aggressive driving conditions. At low temperatures (−7°C), MPFI emissions increased dramatically, matching or exceeding GDI emissions. These findings highlight the need for Gasoline Particle Filters (GPF) and stricter emission controls to meet upcoming standards like China 6 [14]. The study investigated a Dual-Port Injection (DPI) system in a spark-ignition engine with two injectors per cylinder. Wider spray angles improved fuel distribution but increased wall wetting.

The DPI system reduced Brake-Specific Fuel Consumption (BSFC) by an average of 2.8%, with a maximum reduction of 4.6%. Cold-start tests showed fuel economy improvements, though wider sprays increased hydrocarbon emissions [15]. The study converted a spark ignition engine to run on LPG-hydrogen blends using two hydrogen fuelling configurations: separated port inputs and combined port inputs. CFD simulations analyzed the impact of hydrogen injection location on in-cylinder flow and mixture homogenization. Separated LPG-H2 inputs were found optimal based on turbulence and diffusion results. Experiments with varying hydrogen blends (0-20%) showed a 17.5% increase in brake power, a 4.5% improvement in brake thermal efficiency, a 15.1% reduction in CO_2 emissions, and lower hydrocarbon levels at 20% hydrogen addition [16]. The study evaluated the combustion performance of dual injection using n-butanol Direct Injection (DI) and gasoline Port Fuel Injection (PFI) in a single-cylinder SI engine. Compared to gasoline single-injection, dual-injection systems with 80% gasoline PFI-20% n-butanol DI and 50% gasoline PFI-50% n-butanol DI produced higher Indicated Mean Effective Pressure (IMEP) but also increased knock propensity. When n-butanol DI was 80%, its cooling effect reduced knock occurrence.

Dual-injection systems exhibited higher maximum combustion pressures and earlier crank angles but also higher fuel consumption rates. Despite this, n-butanol gasoline dual-injection demonstrated better fuel conversion efficiency [17]. The study explores the impact of Port Dual Injection (PDI) technology on downsized SI engines, focusing on fuel efficiency and emission improvements. Using STAR-CD for CFD analysis, the study examines how fuel injection timing and targeting affect the internal flow and fuel behavior. Experimental validation confirms that optimizing injection conditions reduces liquid fuel film by about 73.04% compared to standard methods, enhancing engine performance and emissions [18]. The study examines the use of Compressed Natural Gas (CNG) in turbocharged Spark Ignition (SI) engines under maximum load conditions. CNG, with a higher octane number, allows for spark timing advancement, improving thermal efficiency compared to gasoline.

However, the maximum load capacity is 4–23% lower due to the port injection system. While CNG combustion produces higher NOx emissions than Gasoline Direct Injection (GDI), it results in lower CO_2 emissions and better combustion efficiency. The limitations and benefits of using CNG in turbocharged engines are discussed [19]. The study explores optimizing hydrogen/gasoline dual-fueled engines to address power loss and NOx emissions. By using AVL

BOOST software for simulation and the Latin Hypercube design of experiments, the study evaluates the impacts of water injection and the Start of Combustion (SOC) modifications. Multi-objective optimization with a genetic algorithm identified optimal parameters that improved Brake Mean Effective Pressure (BMEP) and engine performance without increasing NOx emissions. The results show up to 4.61% improvement in Brake Specific Fuel Consumption (BSFC) and enhanced overall emissions and performance [20]. The study investigates the impact of valve timing variations on performance and methane emissions in natural gas engines, focusing on the effects of intake and exhaust valve adjustments with and without boosting. Experiments showed that excessive advancements in intake valve timing or excessive retardation of exhaust valve timing increased methane slip and reduced engine torque. Optimal valve timings for minimizing methane emissions while meeting EURO-6 standards were identified for engine speeds of 1000–2500 rpm.

The study highlights that valve timing optimization for natural gas engines differs from conventional gasoline engines, particularly at low speeds [21]. The study compares the toxic properties of Particulate Matter (PM) from a conservative gasoline engine using well-ordered gasoline (E0) and a gasoline-ethanol blend (E15). The E15 blend produced similar particle mass and somewhat extra particles by the number associated with E0, but the organic extract from E15 contained higher levels of damaging Polycyclic Aromatic Hydrocarbons (PAHs). Toxicity assessments in human lung cells revealed that both PM extracts caused oxidative stress and affected lipid metabolism and immune response after 4 hours. After 24 hours, E15 specifically dysregulated genes associated with cancer promotion and progression, suggesting that ethanol in gasoline enhances the PAH content and toxicity of PM emissions [22].

The study explores the use of ethanol-gasoline blends in a single-cylinder, four-stroke spark ignition engine to address emissions of NOx, HC, and CO. Ethanol blends tested include 75% ethanol, 25% gasoline, 50% ethanol/50% gasoline, and 25% ethanol, 75% gasoline. Presentation limitations such as detonation effectiveness and brake thermal effectiveness were evaluated, along with emissions of HC, CO, and NOx. The use of ethanol blends is examined as a means to reduce critical emissions and improve engine performance [23]. The study worked on Response Surface Methodology (RSM) with the Design of Experiments (DoE) to enhance the Compression Ratio (CR), engine load, and 1-heptanol percentage in a Spark Ignition (SI) engine. Experiments tested three levels of 1-heptanol (0%, 10%, 20%), CR (6.0:1, 8.0:1, 10.0:1), and engine loads (4, 8, 12 kg). The optimal conditions identified were 10% 1-heptanol, 10.0:1 CR, and 6 kg load, resulting in improved Brake Thermal Efficiency (BTHE) and Brake-Specific Fuel Consumption (BSFC), with CO, CO_2, HC, and NOx emissions also measured. Adding 10% 1-heptanol enhanced BTHE and BSFC, while 20% heptanol improved CO emissions but negatively affected HC and CO_2. Increasing CR to 10.0:1 improved BTHE, BSFC, CO, and HC but increased CO_2 and NOx. The study provides valuable parameters for using 1-heptanol as an alternative fuel in gasoline engines [24]. The utilization of a hydrogen direct injection system featuring outwardly opening poppet valves in small engines for light-duty applications has been investigated.

A comparative analysis between hydrogen direct injection and port fuel injection in a single-cylinder spark ignition engine was conducted to asses performance, emissions and combustion characteristics under varying engine loads, air dilution levels and injection timing conditions. The findings indicate that the DI system enhances efficiency by 0.6 % to 1.1 % relative to PFI. Furthermore, retarding injection timing resulted in a reduction in compression work by 7.6 % at low load and 3.9 % at high load, contributing to a 3.1 %- 3.2 % improvement in indicated specific fuel consumption. These results underscore the advantages of hydrogen DI in optimizing engine performance while mitigating emissions [25].

Additionally, a comparative study examined the performance and emissions of PFI and DI in hydrogen-fuelled spark ignition engines alongside methane and coke oven gas. Computational fluid dynamics simulations were employed to analyze combustion behaviour at optimal spark advance and air-fuel ratios across engine speeds ranging from 2000 to 5000 rpm. The results demonstrated that DI enhances brake power by 40% and volumetric efficiency by 30.6 % compared to PFI while also achieving a 36 % reduction in Nox emissions at λ=1.5 for hydrogen. Moreover, hydrogen exhibited significant fuel consumption reductions of 71.8 % and 67.2 % in comparison to methane and coke oven gas, respectively, attributed to its higher lower heating value per unit mass. These findings reinforce the potential of hydrogen DI systems in advancing combustion efficiency and emission control in spark ignition engines

3. Experimental Setup

The existing naturally aspirated 796 cc, 3-cylinder gasoline SI engine is modified for Sequential Port Fuel Injection (SPFI) and Conventional Manifold Fuel Injection (CMFI) for dual fuel operation. All trials are performed at constant speeds of 2000, 2500, 3000, 3500, and 4000 RPM under Wide-Open Throttle (WOT) conditions with an equivalence ratio (Ø = 1). Separate trials are conducted in SPFI mode and CMFI mode. Conventional fuel injection in the inlet manifold is done by modifying the SPFI by removing the ECU-operated injectors, and the fuel coming from a vaporizer is directly given to the injector installed near the TPMS sensor. Manually, the flow is controlled in CFMI by the flow control valve.

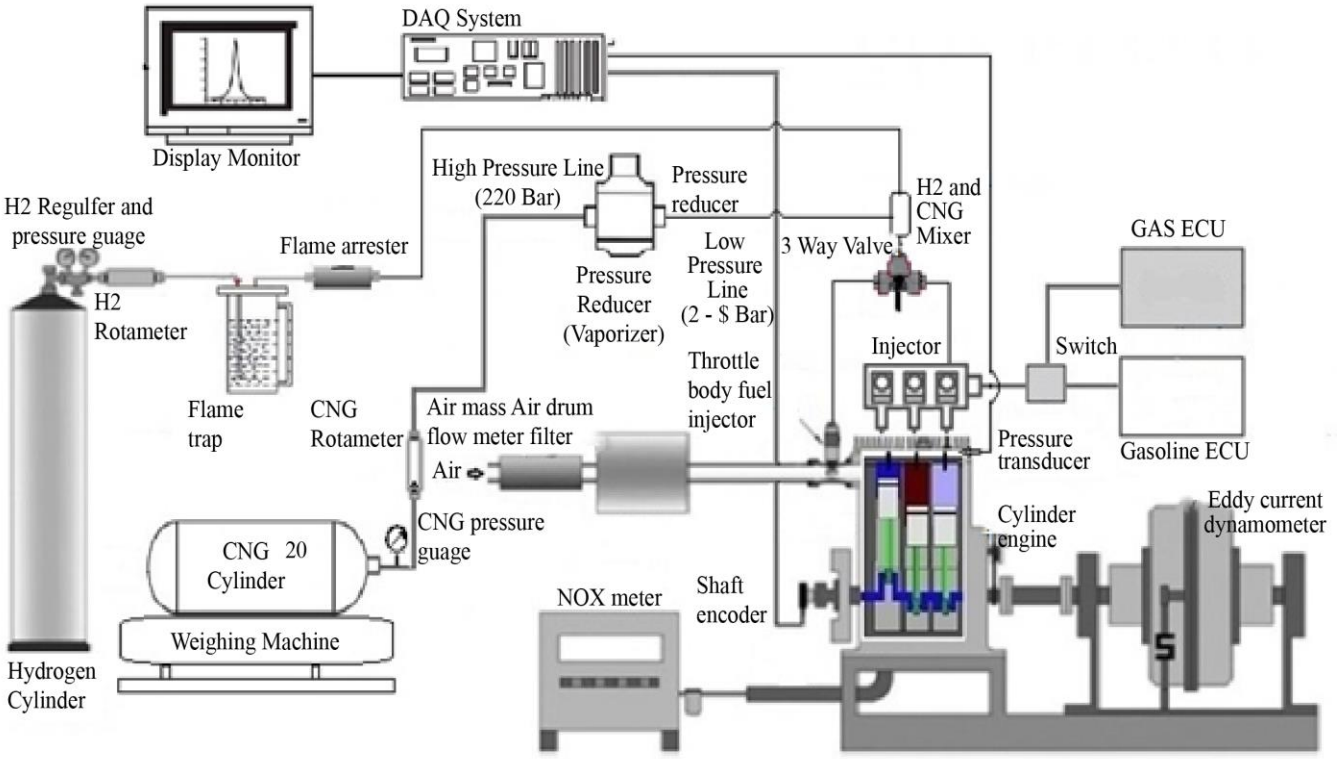

Fig. 1 Experimental setup

During the trials, hydrogen and CNG are mixed online. To prevent backfires, flame traps and flame arrestors are installed on the CNG and hydrogen fuel lines. A 75-litre CNG cylinder at a pressure of 200 bar and a 90-litre hydrogen cylinder at a pressure of 180 bar are used for the trials. The flow pressure in the fuel injection lines is maintained at 2.8 bar to achieve an equivalence ratio of 1. A rotameter is used to measure the fuel flow rate online in litres per minute, and readings are noted every 5 minutes during the trial. A pressure reducer lowers the pressure of CNG from 200 bar to 2.8 bar and hydrogen from 180 bar to 2.8 bar. Hot water from the engine coolant is circulated around the vaporizer (pressure reducer) to prevent icing caused by the pressure drop.

A weighing machine is used to measure the CNG consumption by mass during the trial, verifying the fuel consumption values. The distributor adjusts spark timing at each engine speed to maximize brake torque. The flow rates of CNG and hydrogen are adjusted to achieve the desired air-fuel ratio. Air consumption is measured using the air-box method with a manometer, and fuel consumption is measured using the rotameter. HCNG is supplied to the engine through injectors near the inlet valve in the port fuel injection system and near the inlet manifold in the CMFI system.

A pressure transducer is installed in one cylinder to measure in-cylinder pressure for combustion calculations. Cooling water circulation is made around it to maintain the temperature within limits. An eddy current dynamometer is used to measure the load through a strain gauge during the trials. The circulated cooling water absorbs the heat generated by the magnetic field during loading. The spark advance for HCNG blends is adjusted using the distributor, and spark timing is recorded with a timing light.

RTD thermocouple is used to measure exhaust temperature, and an O_2 sensor is used to measure exhaust oxygen content. An AVL 5-gas analyzer is used online to measure exhaust CO, CO_2, HC, O_2 and Nox in the exhaust during trial. HC, CO and NOx are measured in Parts Per Million (PPM), while CO_2 and O_2 are measured in percentage by volume. % Volume and PPM values are converted to grams per kilowatt-hour (g/kW.hr) through theoretical calculations. All trials are conducted according to SAE standards.

Cooled Exhaust Gas Recirculation (EGR) is used to control NOx at higher loads and speeds. Throughout the trials, the engine temperature is maintained at 80°C for steady-state readings by using a separate cooling system. Full throttle is kept constant during the trials, and engine speed is varied by adjusting the load on the dynamometer.

Ni-DAQ software is used to record data from the pressure transducer, converting it into Cumulative Heat Release Rate (CHRR), Net Heat Release Rate (NHRR), Start of Ignition (SI), Mass Fraction Burned (MFB) and Maximum Pressure

(Pmax). TAMMONA software is used to measure fuel injection pressure and the pulse width of the injector. Three HCNG injectors are fitted near the inlet valve, close to the gasoline injector. For conventional fuel injection, one injector is placed near the inlet manifold, close to the Manifold Absolute Pressure (MAP) sensor. The timing gear is calibrated, and spark timing is measured with a timing light during the trials. Online Pressure-Crank Angle (P-Θ) analysis is used for combustion analysis.

The air-box method is employed to measure air consumption using a water manometer. Each trial lasts for 5 minutes under steady-state conditions. Friction power is calculated by the Morse test for constant speeds of 2000, 2500, 3000, 3500, and 4000 rpm. During the trials, the Compression Ratio (CR) of 9.2 and an equivalence ratio of 1 are maintained at all speeds under WOT conditions. Strain gauge is used to measure the load on the Eddy current dynamometer.

The engine setup is equipped with the following sensors:

1. Oxygen sensor
2. MAP sensor
3. TPS sensor
4. RPM sensor
5. Inlet Air Temperature sensor

The observations recorded from the experimental setup are:

1. Pressure-Crank Angle Diagram (P-Θ)
2. Load
3. Exhaust Temperature
4. Engine Speed
5. Mass of Air Consumption
6. Mass of Fuel Consumption
7. CO, HC, CO_2, O_2, and NOx levels.

4. Result and Discussion

4.1. Brake Power

Due to gaseous fuel the charge intake and power output reduces due to lower volumetric efficiency as it is used in dedicated gasoline bi-fuel engine. In SPFI the power output is more compared to Conventional Manifold Injection (CMI) at all speed. In naturally aspirated engine CMI the charge intake reduces which reduces power output. Maximum power of 12.5 kW is observed for SPFI and it reduced to 11.38 kW in CMFI. 8.9 % drop in power is observed in CMI compared to SPFI.

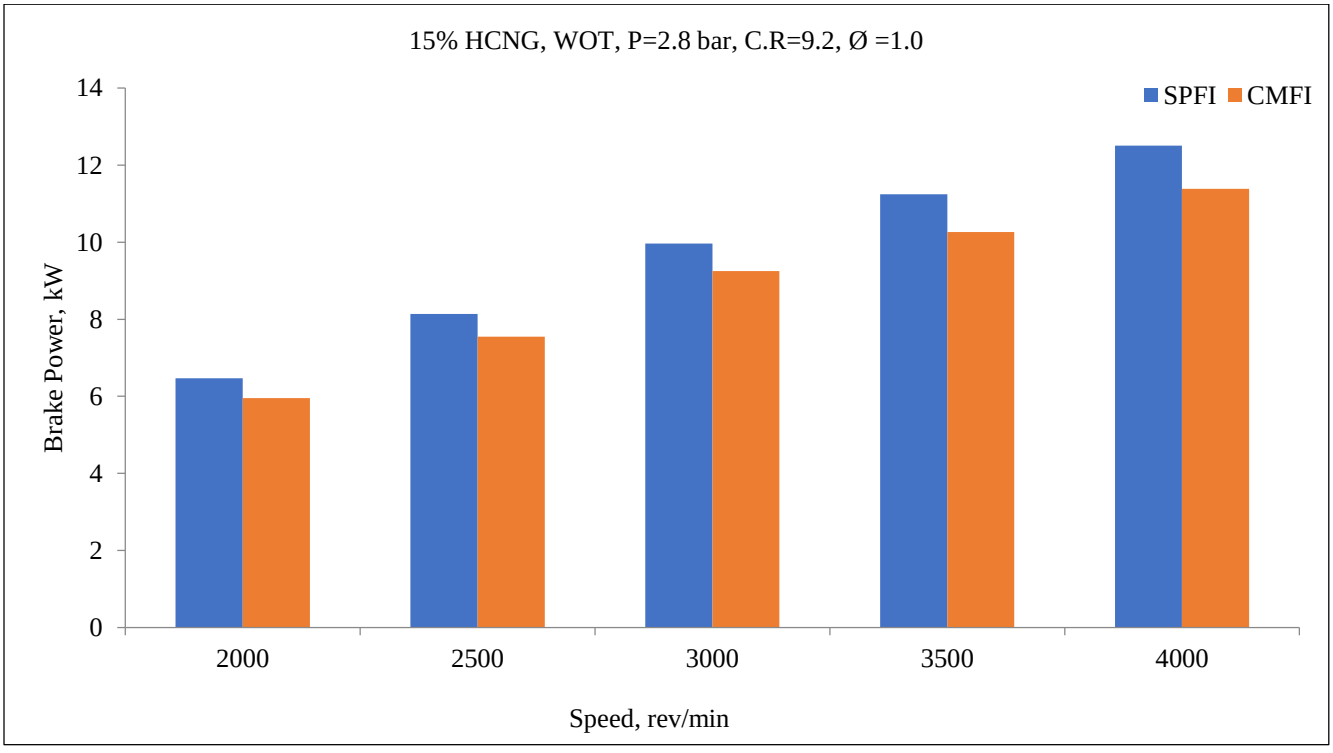

Fig. 2 Speed Vs Brake power

4.2. Brake Thermal Efficiency

The fuel economy of the engine is determined by its Brake Thermal Efficiency (BTE). In gaseous fuels, BTE decreases due to higher fuel consumption. In dual-fuel combustion engines, the thermal efficiency in SPFI mode is observed to be 16.06%, while in Conventional Manifold Fuel Injection (CMFI) mode, it reduces to 13.51% at a speed of 4000 RPM. This represents a drop of 15.87% in BTE for CMFI compared to SPFI. BTE increases with engine speed and reaches its maximum at 3500 RPM. However, it decreases as the speed continues to rise due to incomplete combustion. SPFI offers more precise fuel injection based on load and speed, which helps improve BTE.

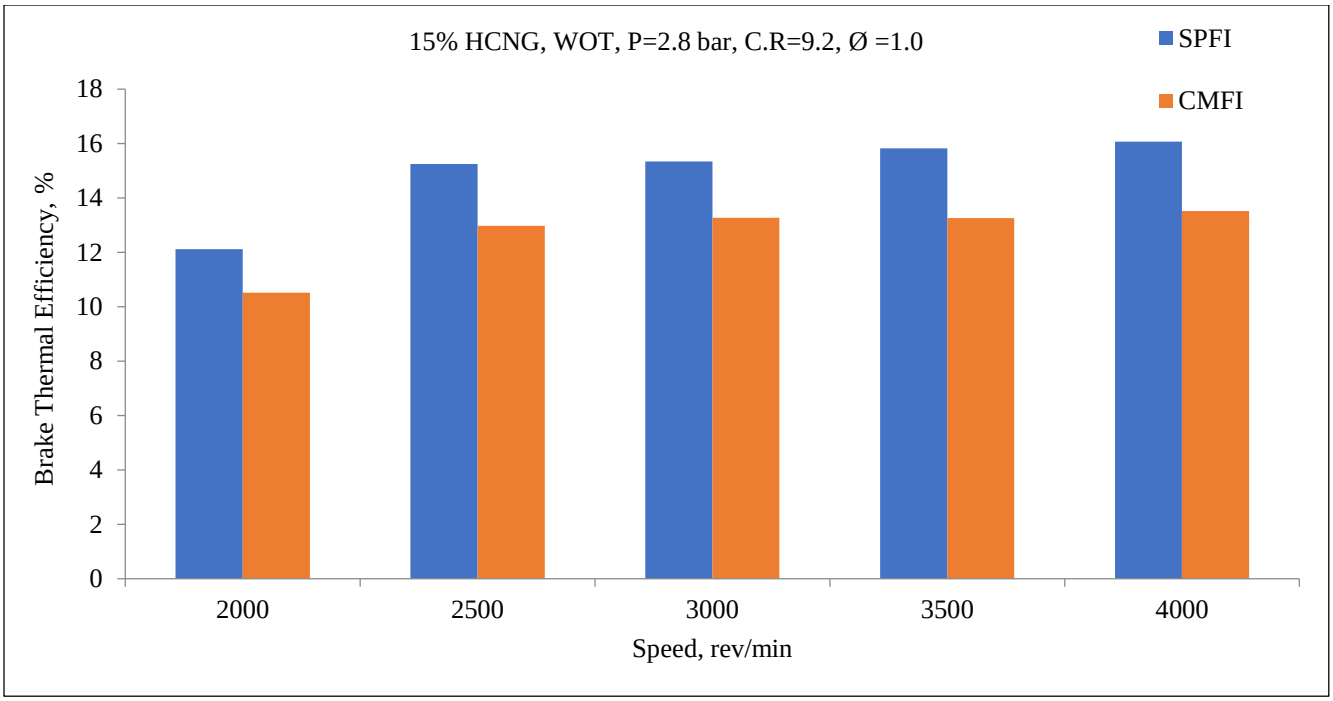

Fig. 3 Speed Vs Brake thermal efficiency

4.3. Volumetric Efficiency

The cylinder's charge intake is shown by volumetric efficiency. It diminishes as the speed and ambient temperature rise. When it comes to gaseous fuel, it decreases because of the fuel's decreased density. The volumetric efficiency of the HCNG blend was shown to decline as speed increased. Because each fuel injector in an SPFI has a pressure of 2.8 bar, it is more than in a CMFI. Due to the single injector and natural aspiration of fuel during the suction stroke, it decreases with CMFI. With SPFI, the volumetric efficiency is measured at 4000 rpm and decreases to 84.01% at that speed. Because there was less time for suction and the cylinder was hotter, it dropped by 20% at 4000 rpm.

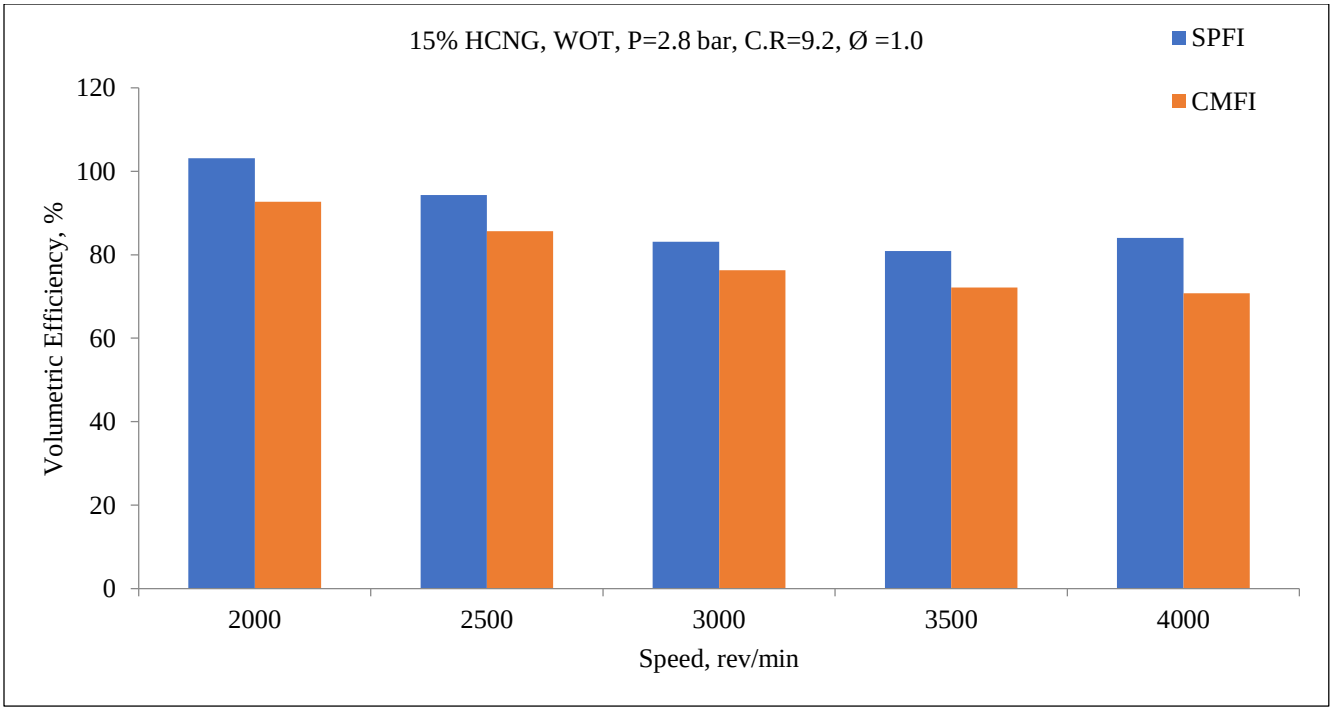

Fig. 4 Speed Vs Volumetric efficiency

4.4. Carbon Monoxide

CO is minimal at optimum speed and increases at lower and higher speeds; at lower speeds due to less availability of oxygen and at higher speeds due to incomplete combustion, CO emission increases. Due to hydrogen addition, CO emission decreases at all speeds compared to gasoline and pure CNG. In HCNG blends, CO emissions are more at a lower speed and decrease with an increase in speed. At a speed of 2000 rpm with CMFI, CO emissions are 53.41 kg/kW.hr and decrease by 19.17 % to 43.17 gm/kW.hr in SPFI due to fuel injection in each cylinder separately and precisely at all speeds.

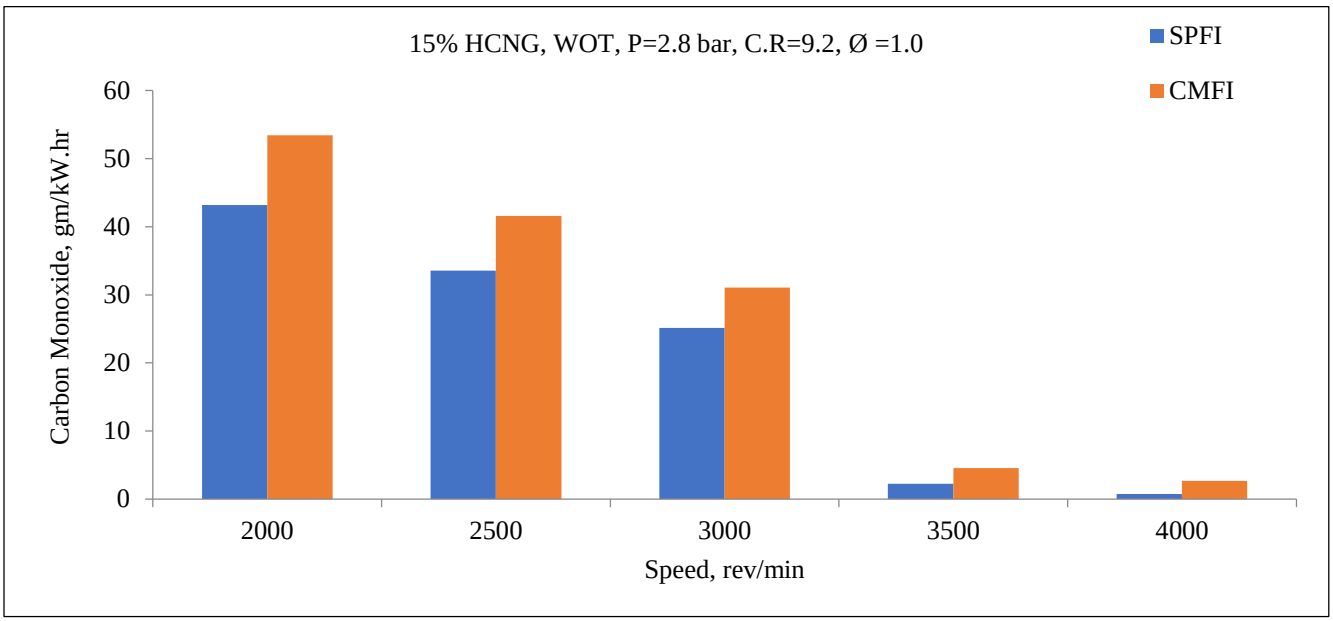

Fig. 5 Speed Vs Carbon monoxide

4.5. Hydrocarbon

Hydrocarbon in exhaust indicates incomplete combustion and reduces thermal efficiency due to loss of charge in exhaust. It pollutes the environment and living beings. It enters the blood during inhaling and forms dizziness in the body as it absorbs oxygen in the blood. They are minimal at lower speeds and increase with speed due to the minimum time available for combustion. The presence of hydrocarbon in the exhaust increases the chances of backfire during valve overlap. With SPFI, it reduced by more than 50 % compared to CMFI due to complete combustion.

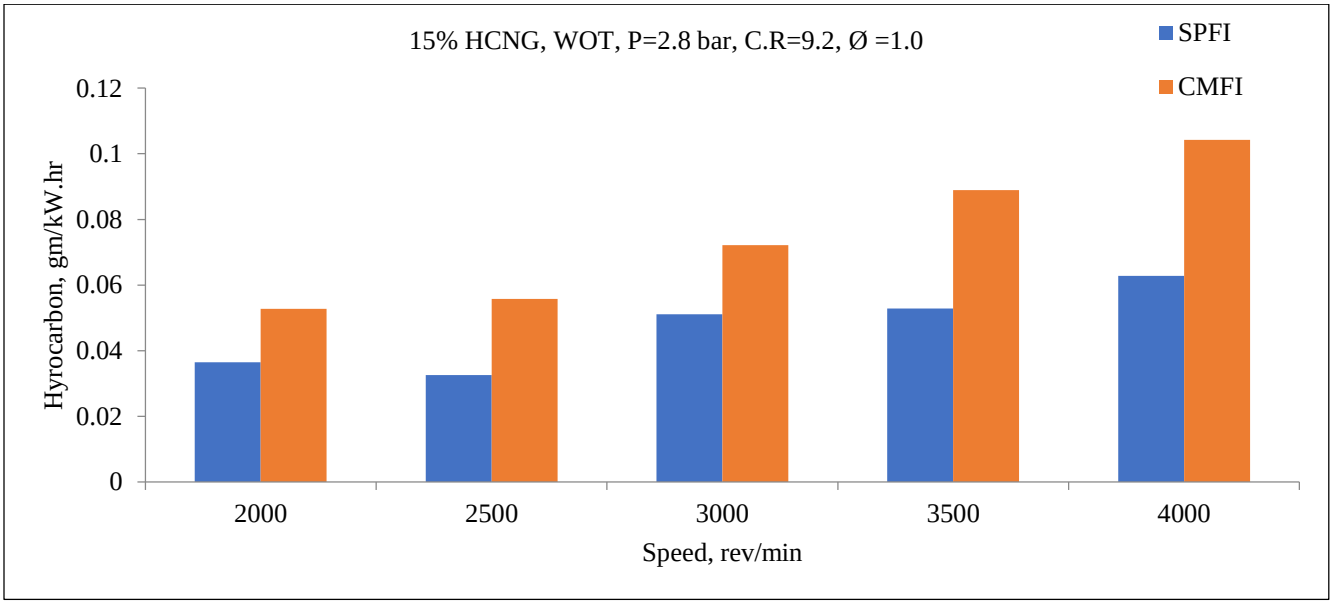

Fig. 6 Speed Vs Hydrocarbon

4.6. Oxides of Nitrogen

NOx is formed at higher temperatures (above 1200 o C) and complete combustion in the combustion chamber. It is 54 5 higher in SPFI compared to CMFI due to more charge intake through the injector. NOX of 9.6 gm/kW.hr is observed in SPFI and 6.3 gm/kW.hr for CMFI at 4000 rpm. Nox and Power output increases at MBT spark timing.

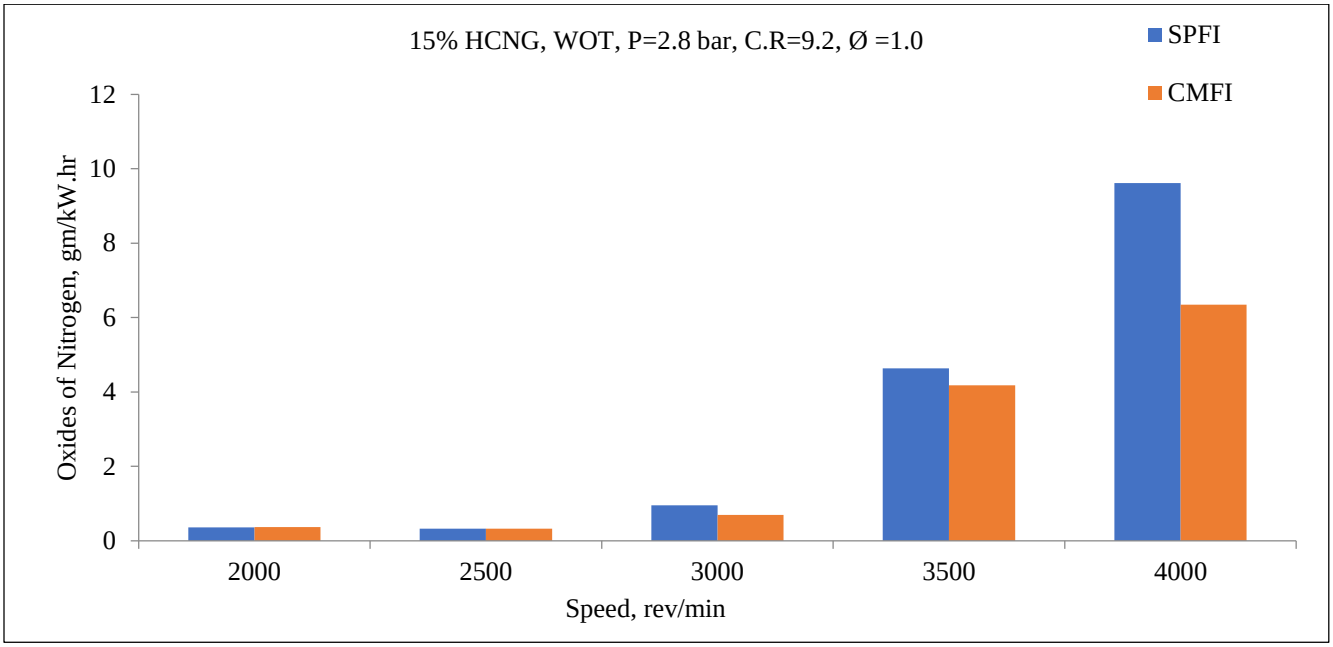

Fig. 7 Speed Vs Oxides of Nitrogen

4.7. Exhaust Temperature

Exhaust temperature increases with an increase in speed due to the higher calorific value of hydrogen. Higher temperatures increase NOx and engine life. There is a chance of valve damage and engine ceasing. Texh is maximum at 4000 rpm, and further, it decreases due to incomplete combustion. A maximum temperature of 488 o C is observed for a 10 % HCNG blend in SPFI, and it decreased to 380 o C with CMFI. There is a drop in temperature of 22.13 % due to a reduction in charge intake of the Air fuel mixture in CMFI.

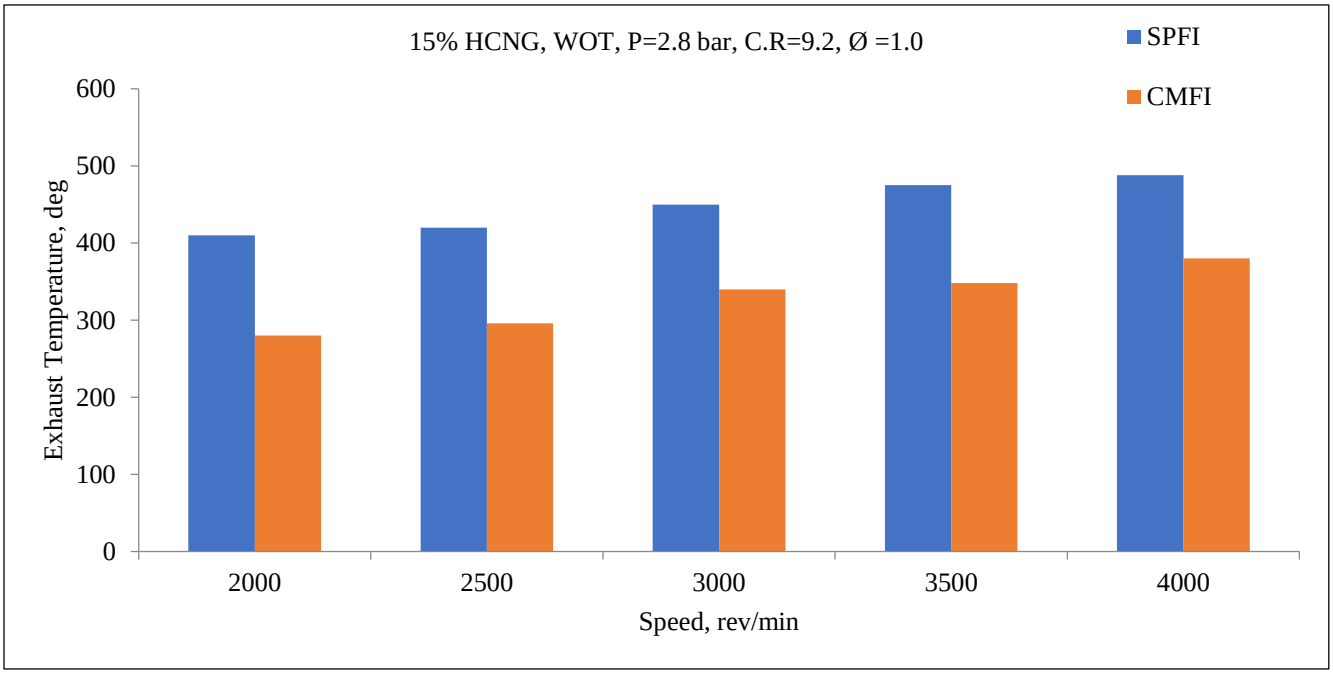

Fig. 8 Speed Vs Exhaust temperature

4.8. Brake Mean Effective Pressure

Brake Mean Effective Pressure (BMEP) versus engine speed for SPFI and CMFI during 15% HCNG operation. SPFI, at all speeds, has higher BMEP compared to CMFI owing to more uniform charge distribution and combustion efficiency. BMEP goes up with speed, peaking at 3000 RPM, before dropping slightly. At 4000 RPM, CMFI has the lowest BMEP due to reduced charge intake and inhomogeneous air-fuel mixing. The increased flame speed of HCNG blends increases combustion, which increases BMEP in both instances, with SPFI showing better performance.

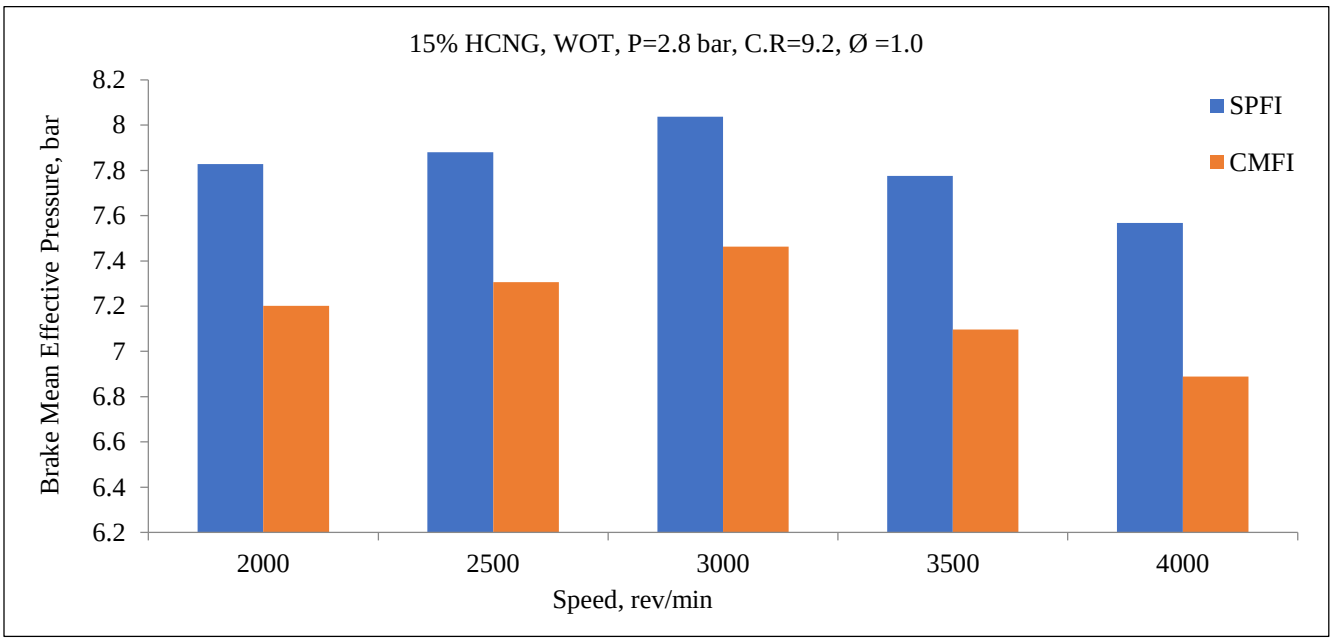

Fig. 9 Speed Vs Brake mean effective pressure

4.9. Brake-Specific Energy Consumption

Brake-specific fuel consumption is maximum at lower speeds due to insufficient O_2 and at higher speeds due to the time limit for combustion. With HCNG blends, BSEC decreases at all speeds due to enhancements in flame speed during combustion. More the flame speed, the lower the chances of detonation. At 4000 rpm with SPFI, 20.60 gm/kW.hr of fuel consumption is observed, and it increased by 20.32% in CMFI less charge intake and non-uniform distribution of charge in the cylinder.

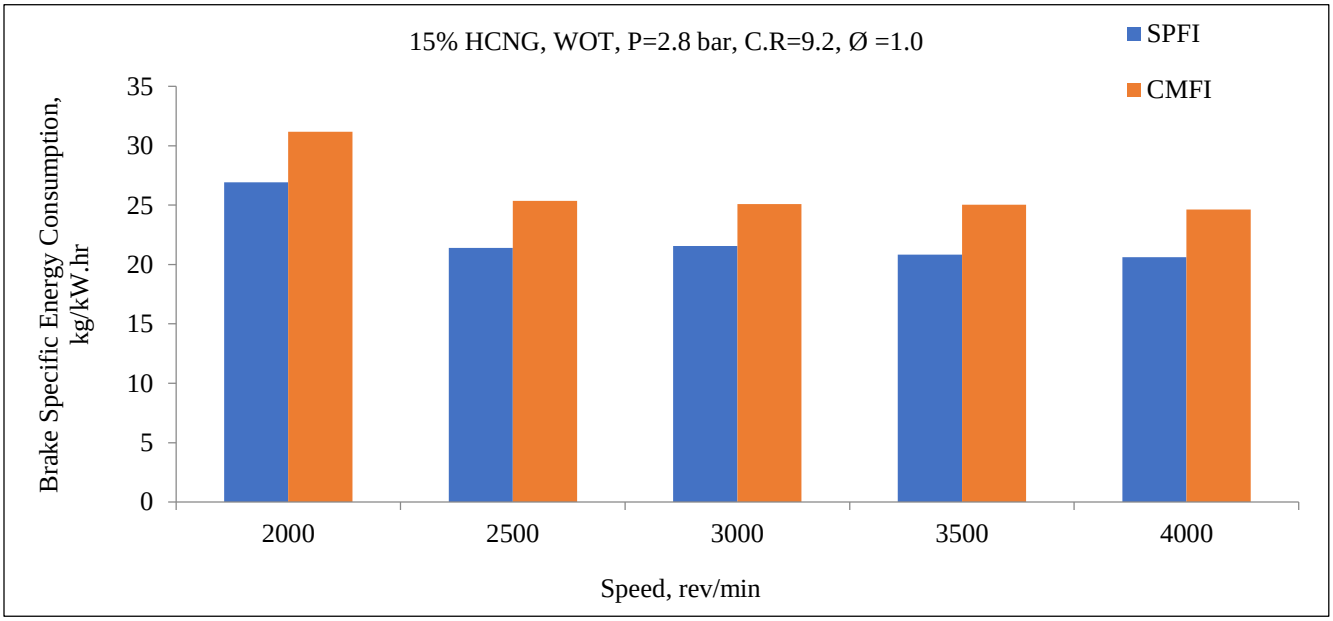

Fig. 10 Speed Vs Brake specific energy consumption

4.10. Brake Specific Fuel Consumption

Figure 11 shows that BSFC decreases with an increase in speed due to complete combustion. A minimum BSFC of 0.4 kg/kW.hr is observed for the Sequential Port Fuel injection system at 2500 rpm.

SPFI is more beneficial due to precise injection in each cylinder at optimum timing during combustion. BSFC increases at lower speeds due to low turbulence and non-uniform mixing of charge with air, which increases HC and CO emissions.

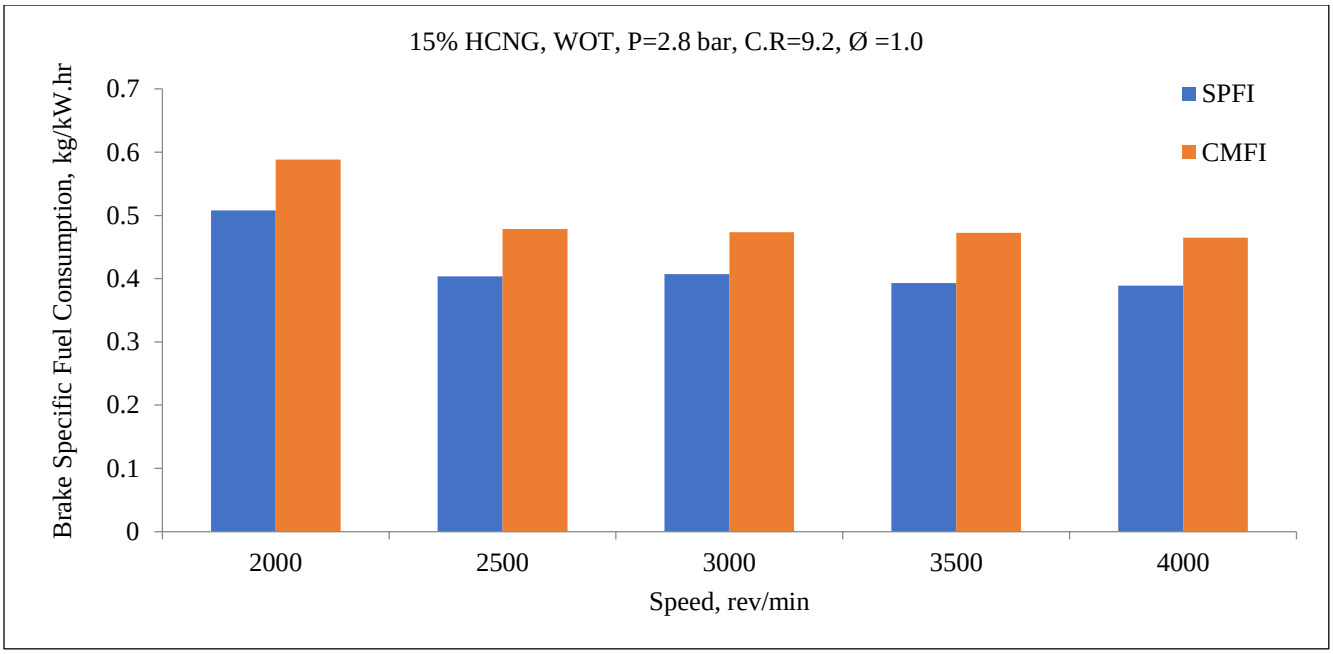

Fig. 11 Speed Vs Brake specific fuel consumption

4.11. Cylinder Maximum Pressure

With 10 % HCNG blends, the peak pressure increases compared to CNG combustion pressure. The addition of hydrogen enhances the lean limit and increases the combustion temperature. Complete combustion is observed with minimum O_2 in the exhaust. Pmax of 35 bar is detected with SPFI in 10 % HCNG blend and it decreased to 27 bar with CMFI. The drop of 22.63 % in peak pressure is observed with CMFI due to incomplete combustion and non-uniform distribution of charge at higher speed.

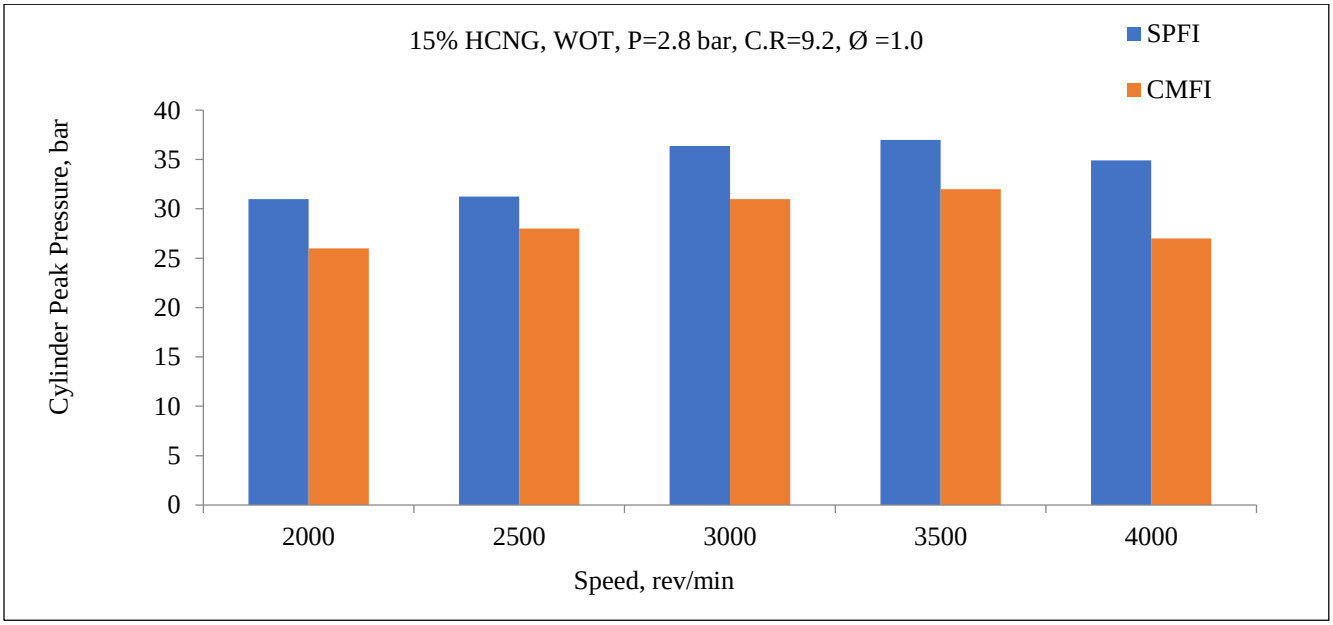

Fig. 12 Speed Vs Cylinder peak pressure

4.12. Combustion Analysis

4.12.1. Combustion Duration

Combustion investigation shows that hydrogen improves rapid combustion. The fuel with optimum HCNG blends and spark timing shows the best characteristics for in-cylinder pressure, with low expansion cylinder temperatures and moderate combustion peak temperatures. Losses from incomplete combustion decrease as the hydrogen fraction rises. Once the hydrogen proportion reaches 10%, the incomplete combustion losses start to decline once more. When hydrogen is added, partial combustion losses are much reduced compared to pure CNG. As the amount of hydrogen added increases, real combustion losses likewise decrease. The limited time of combustion is the cause of real combustion losses, which are only zero in the event of instantaneous combustion at TDC. Accelerated combustion is demonstrated by decreasing real combustion losses. As the hydrogen proportion rises, the wall heat losses increase noticeably. The higher wall heat losses can be attributed to two main factors. In addition to raising the temperatures inside the cylinder, hydrogen in the fuel shortens the distance needed for the flame to quench. The flame front, which is noticeably warmer, gets closer to the cylinder wall. Engine efficiency might be increased, and cylinder wall heat losses could be decreased with a dedicated design for the combustion chamber. Reducing the compression ratio has the potential to mitigate heat losses as well (the flame eventually reaches the walls).

4.12.2. Flame Development Duration

The time interval between the spark release and the point at which 10 % of the cylinder mass has burned is represented by the flame development duration. The early flame growth rate accelerates with an increase in hydrogen input, reducing the flame development period.

4.12.3. Maximum Brake Torque Spark Timing (MBT-ST)

Spark Advance timing increases with an increase in speed, and it is more for CNG due to its slow flame speed. Hydrogen addition improves CNG flame speed with a decrease in spark timing. MBT-ST improves power output and brake thermal efficiency. CNG has a higher octane number, which reduces the knock tendency of the engine and is more efficient at a higher compression ratio (Figure 13).

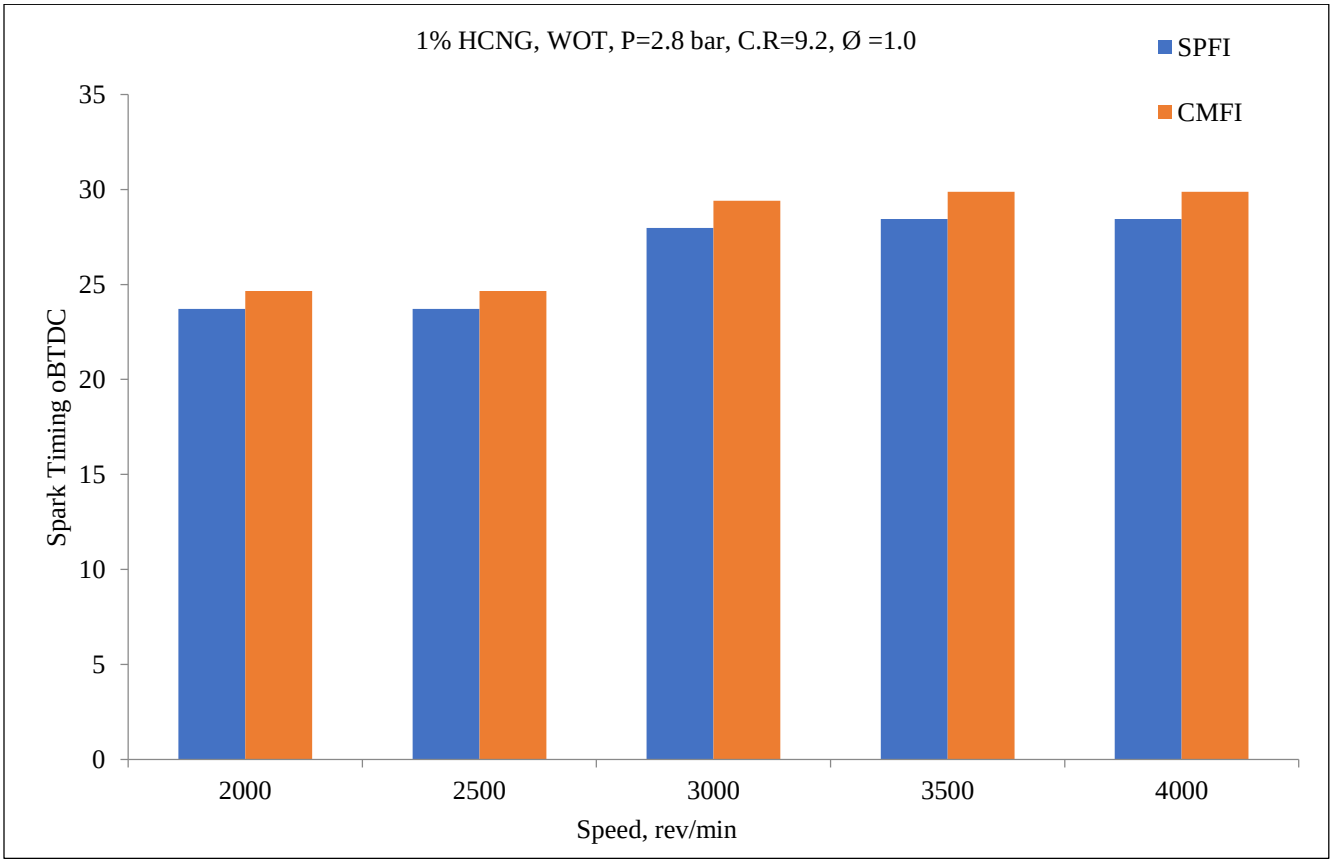

Fig. 13 Speed Vs Spark timing

4.12.4. Cylinder Maximum Pressure

As hydrogen is added, cylinder peak pressure rises, and trends towards TDC result in longer combustion times and faster flames. The maximum peak pressure is reached at 3000 rpm for a cylinder with a 5% hydrogen addition (Figures 14,and 15).

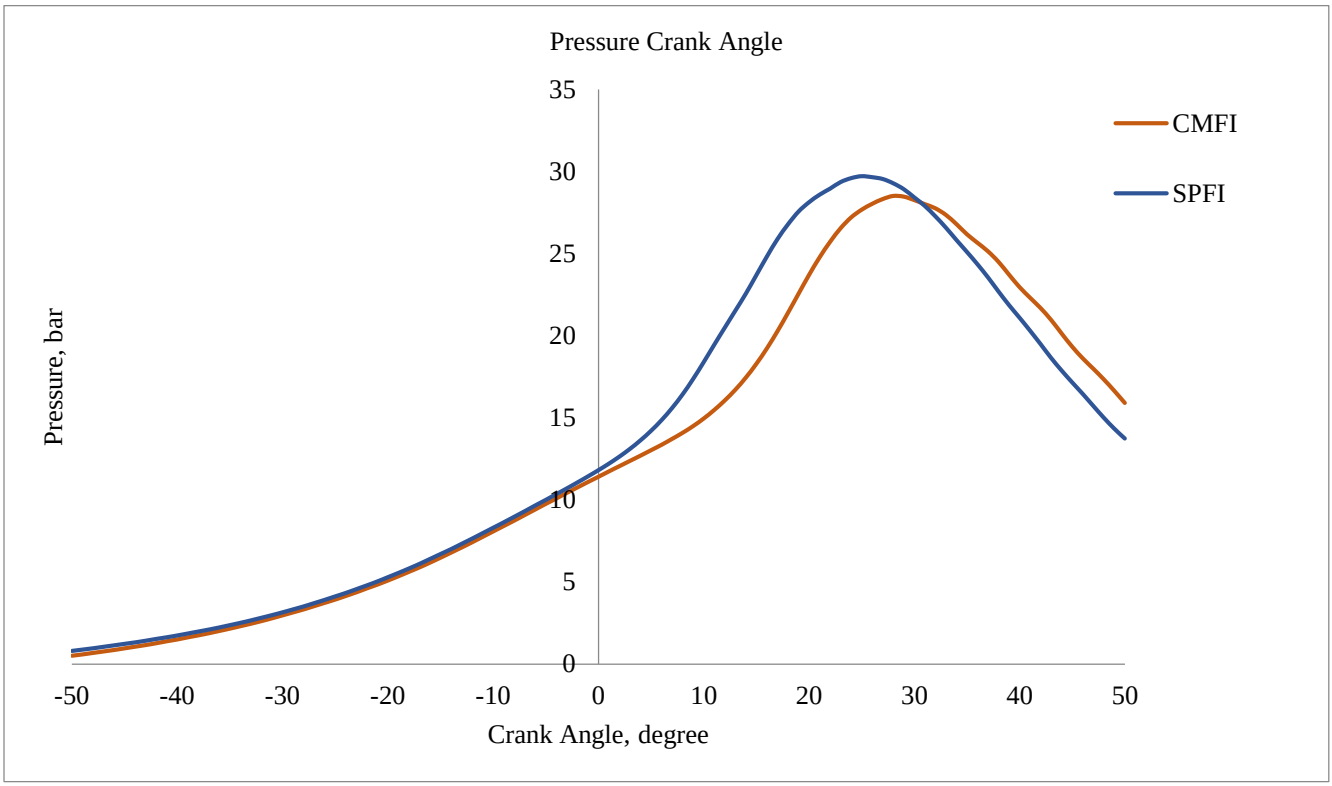

Fig. 14 Speed Vs Pressure

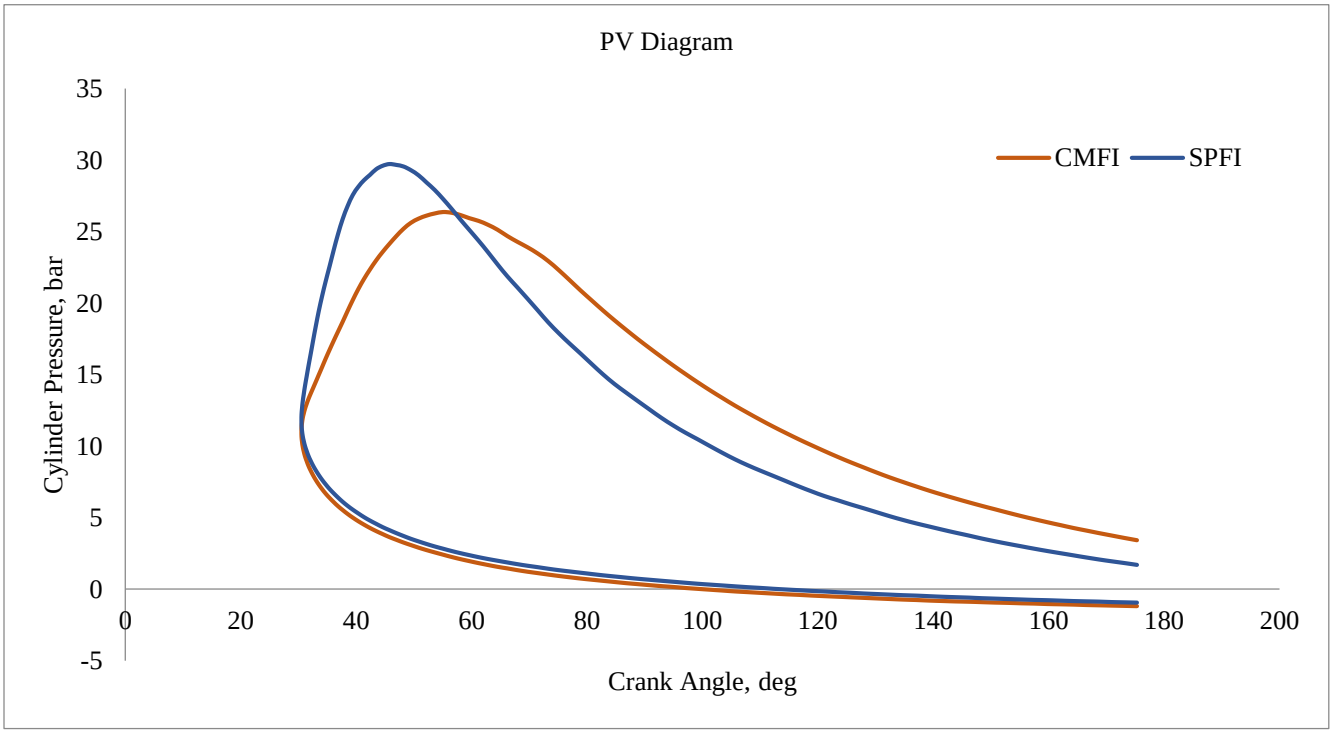

Fig. 15 Speed Vs Cylinder pressure

4.12.5. Heat Release Rate

The heat release rates and cumulative heat release rates of the fuel mixes are shown in Figures 16 and 17. Lower burning velocity causes the maximum heat release rate to drop and the crank angle of the maximum heat release rate to be delayed.

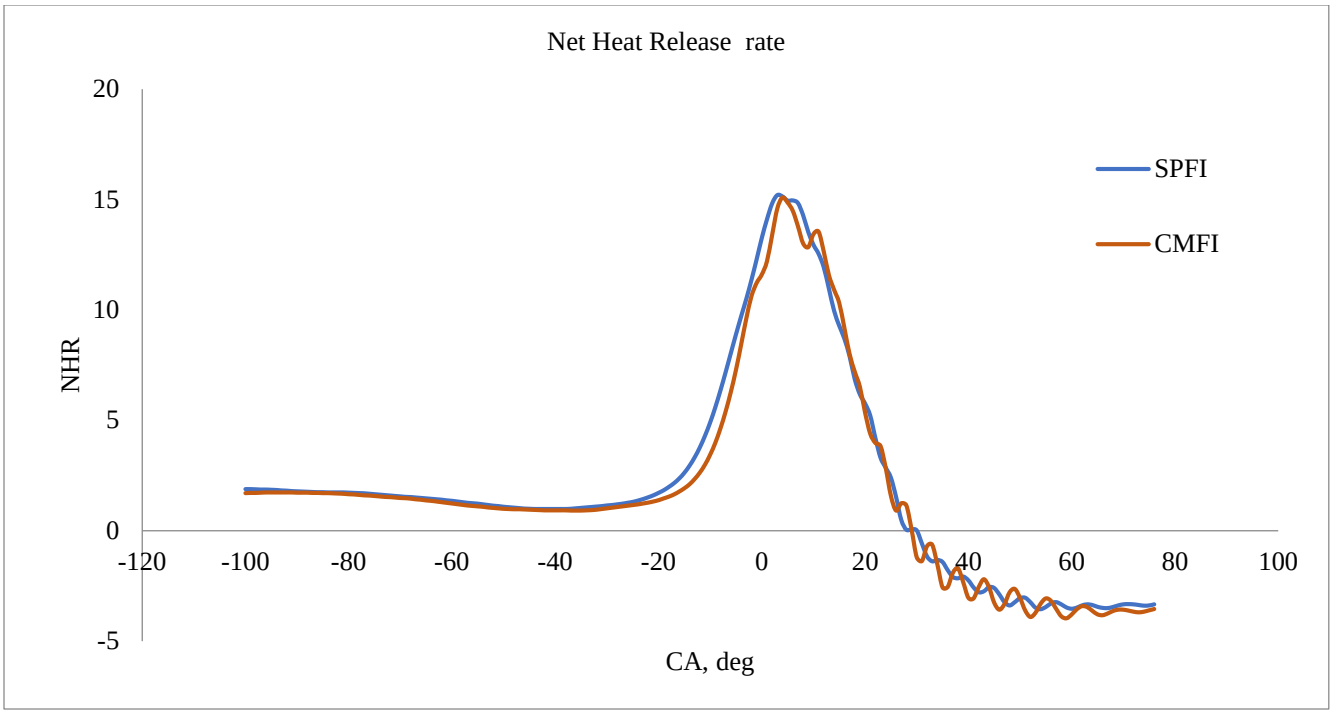

Fig. 16 Speed Vs Net heat release rate

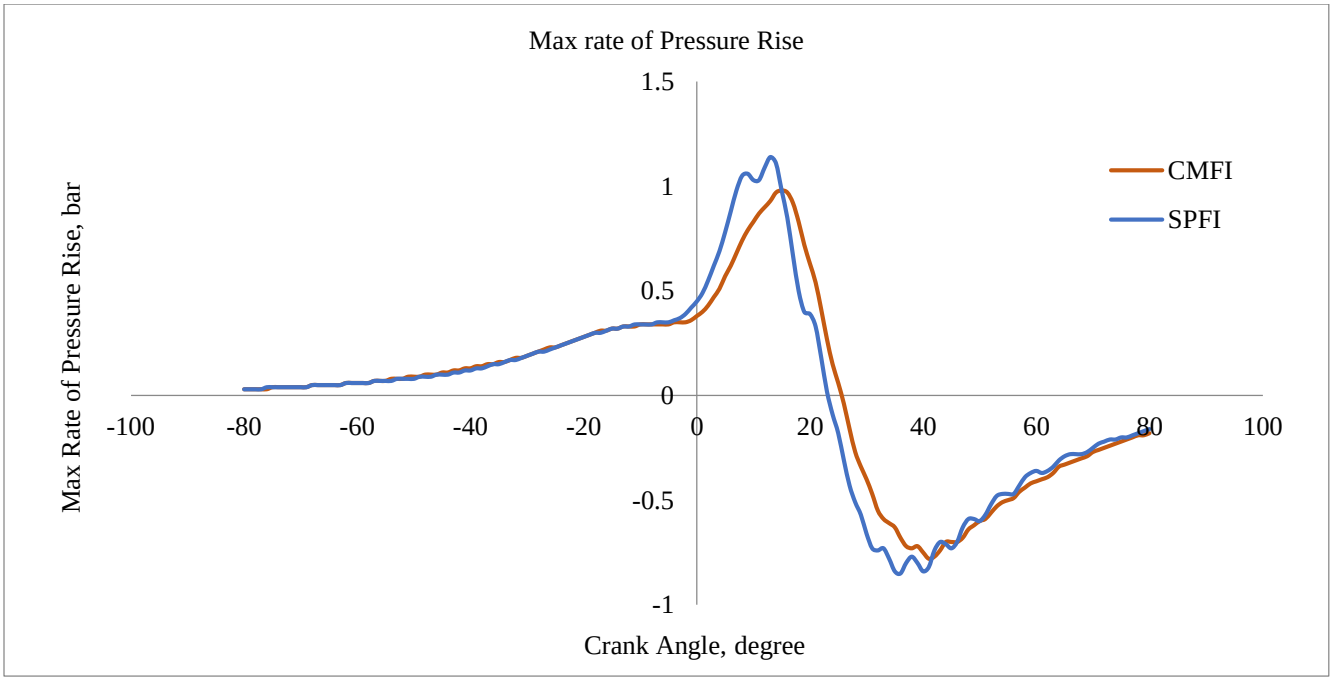

Fig. 17 Speed Vs Maximum rate of pressure rise

4.12.6. Cycle by Cycle Variation

The figure illustrates how the addition of hydrogen enhanced combustion stability. This is so that combustion can be finished in the allotted time due to hydrogen's faster flame speed. Higher hydrogen blending rates result in a greater improvement in COV_{IMEP} because the stoichiometric mixture's laminar flame speed is proportionate to the hydrogen component. However, the CNG-SI engine has a significant cycle-by-cycle variance problem that reduces engine power output and increases fuel consumption due to its sluggish burning velocity and poor lean-burn capabilities. The COV_{IMEP} varies for 10% H2 fuel blends of hydrogen and CNG; as shown in Figure 18, COVIMEP has a declining trend as the hydrogen proportion rises.

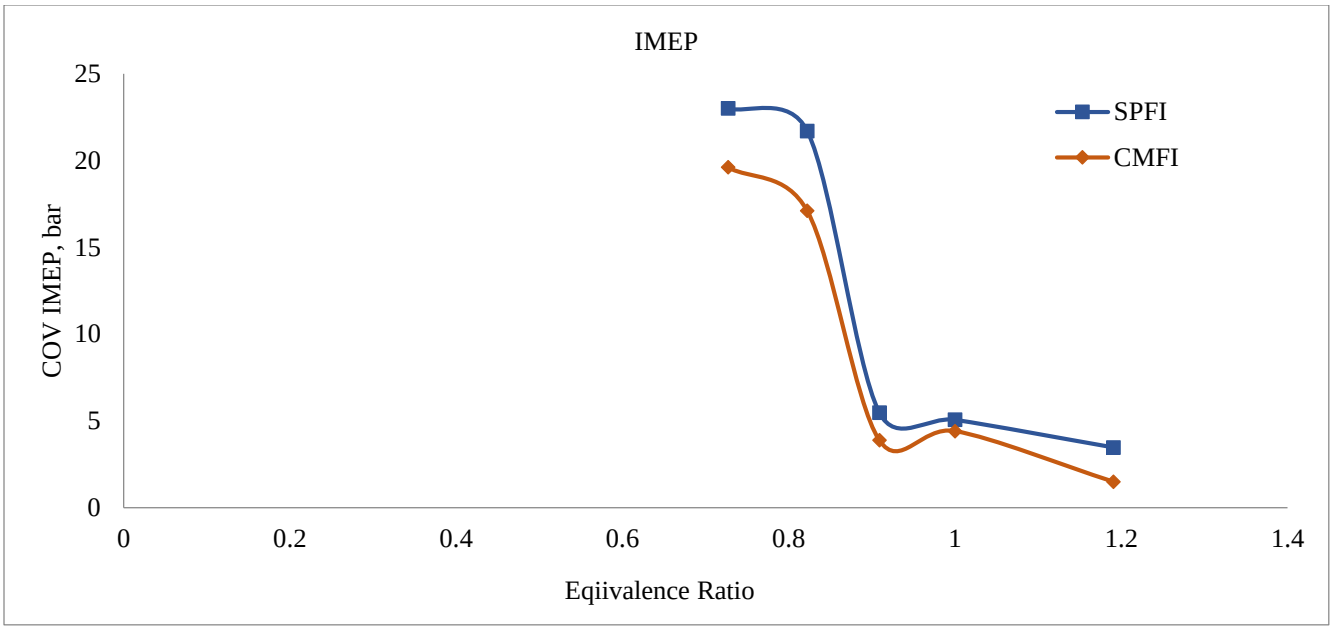

Fig. 18 Speed Vs COV_{IMEP}

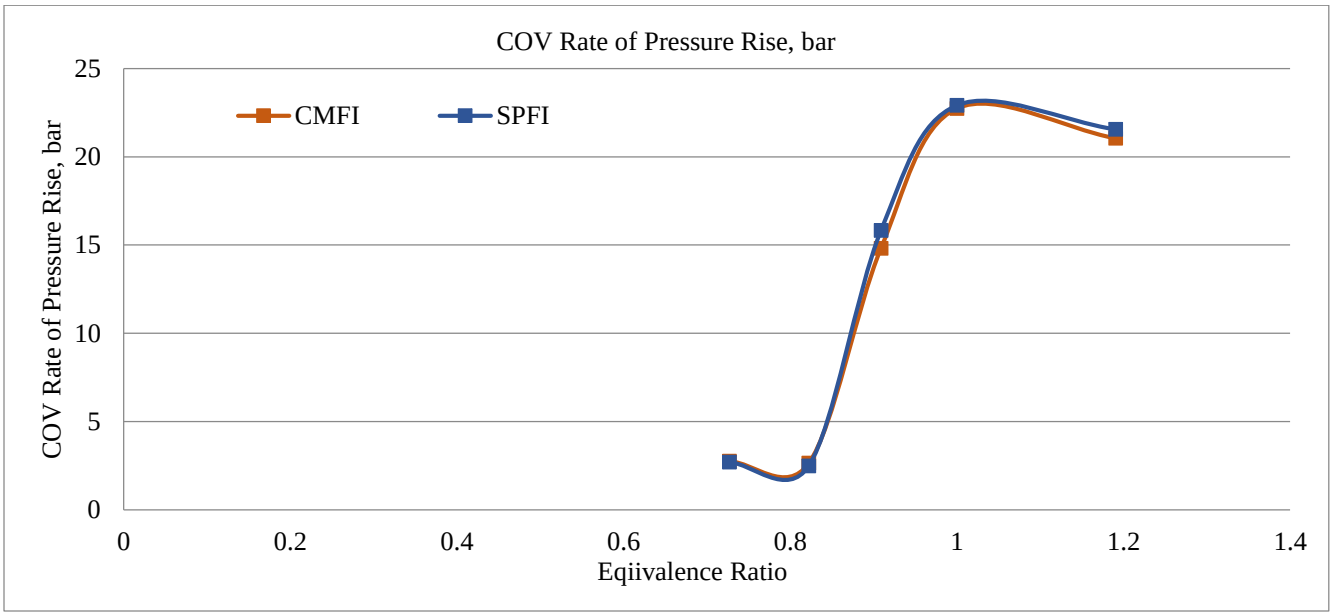

Fig. 19 Speed Vs COV rate of pressure rise

The inclusion of hydrogen can reduce cycle-by-cycle fluctuations. Because natural gas burns at a low velocity, there are significant cycle-by-cycle changes. With an increase in hydrogen proportion, cycle-by-cycle variability decreases even if adding hydrogen to natural gas can enhance burning velocity and minimize misfire and/or partial burning cycles.

Consequently, it is reasonable to anticipate little cycle-by-cycle variance and low-temperature gas engine combustion when using a natural gas and hydrogen blend. Moreover, accelerating an engine will reduce COVIMEP as the turbulence in the cylinder is enhanced (Figure 19).

5. Conclusion and Future Scope

5.1. Conclusions

This study demonstrates that Sequential Port Fuel Injection (SPFI) significantly outperforms Conventional Manifold Fuel Injection (CMFI) in a dual-fuel engine running on 10% HCNG blends. SPFI improves brake thermal efficiency (16.06 % vs 13.51 %), volumetric efficiency and combustion characteristics while reducing CO and HC emissions. However, it leads to higher Nox emissions (9.6 gm/kW.hr vs 6.3 gm/kW.hr) and increased exhaust temperature (488ºC vs 380ºC). SPFI also archives lower Brake-Specific Fuel Consumption (BSFC) and higher peak

cylinder pressure (34.9 bar vs 27 bar), which contribute to enhanced performance. While SPFI proves to be the superior injection strategy, further optimization is required to mitigate Nox emissions and thermal stresses for long-term engine durability.

5.2. Future Scope

- Trials on Direct Injection of HCNG Blends can be studied for performance and emission parameters.
- Effects of compression ratio on HCNG blends can be observed for combustion parameters.

References

[1] Adrian Irimescu, "Fuel Conversion Efficiency of a Port Injection Engine Fueled with Gasoline–Isobutanol Blends," *Energy*, vol. 36, no. 5, pp. 3030-3035, 2011. [CrossRef] [Google Scholar] [Publisher Link]

[2] Muhammad Imran Khan et al., "Research Progress in the Development of Natural Gas as Fuel for Road Vehicles: A Bibliographic Review (1991-2016)," *Renewable and Sustainable Energy Reviews*, vol. 66, pp. 702-741, 2016. [CrossRef] [Google Scholar] [Publisher Link]

[3] Miguel R. Oliveira Panao, Antonio L.N. Moreira, and Diamantino F.G. Durao, "Effect of a Cross-Flow on Spray Impingement with Port Fuel Injection Systems for HCCI Engines," *Fuel*, vol. 106, pp. 249-257, 2013. [CrossRef] [Google Scholar] [Publisher Link]

[4] Gang Lv et al., "Comparison of Number, Surface Area and Volume Distributions of Particles Emitted from a Multipoint Port Fuel Injection Car and a Gasoline Direct Injection Car," *Atmospheric Pollution Research*, vol. 5, no. 4, pp. 753-758, 2014. [CrossRef] [Google Scholar] [Publisher Link]

[5] Yuan Zhuang, and Guang Hong, "Effects of Direct Injection Timing of Ethanol Fuel on Engine Knock and Lean Burn in a Port Injection Gasoline Engine," *Fuel*, vol. 135, pp. 27-37, 2014. [CrossRef] [Google Scholar] [Publisher Link]

[6] Bo Yang et al., "Parametric Investigation of Natural Gas Port Injection and Diesel Pilot Injection on the Combustion and Emissions of a Turbocharged Common Rail Dual-Fuel Engine at Low Load," *Applied Energy*, vol. 143, pp. 130-137, 2015. [CrossRef] [Google Scholar] [Publisher Link]

[7] Yuhan Huang, Guang Hong, and Ronghua Huang, "Numerical Investigation to the Dual-Fuel Spray Combustion Process in an Ethanol Direct Injection Plus Gasoline Port Injection (EDI + GPI) Engine," *Energy Conversion and Management*, vol. 92, pp. 275-286, 2015. [CrossRef] [Google Scholar] [Publisher Link]

[8] F. Catapano et al., "A Comprehensive Analysis of the Effect of Ethanol, Methane and Methane-Hydrogen Blend on the Combustion Process in a PFI (Port Fuel Injection) Engine," *Energy*, vol. 88, pp. 101-110, 2015. [CrossRef] [Google Scholar] [Publisher Link]

[9] Peng Geng, Hui Zhang, and Shichun Yang, "Experimental Investigation on the Combustion and Particulate Matter (PM) Emissions from a Port-Fuel Injection (PFI) Gasoline Engine Fueled with Methanol–Ultralow Sulfur Gasoline Blends," *Fuel*, vol. 145, pp. 221-227, 2015. [CrossRef] [Google Scholar] [Publisher Link]

[10] Yong Qian et al., "Enabling Dual Fuel Sequential Combustion Using Port Fuel Injection of High Reactivity Fuel Combined with Direct Injection of Low Reactivity Fuels," *Applied Thermal Engineering*, vol. 103, pp. 399-410, 2016. [CrossRef] [Google Scholar] [Publisher Link]

[11] Yuhan Huang, and Guang Hong, "Investigation of the Effect of Heated Ethanol Fuel on Combustion and Emissions of an Ethanol Direct Injection Plus Gasoline Port Injection (EDI + GPI) Engine," *Energy Conversion and Management*, vol. 123, pp. 338-347, 2016. [CrossRef] [Google Scholar] [Publisher Link]

[12] Rencheng Zhu et al., "Tailpipe Emissions from Gasoline Direct Injection (GDI) and Port Fuel Injection (PFI) Vehicles at Both Low and High Ambient Temperatures," *Environmental Pollution*, vol. 216, pp. 223-234, 2016. [CrossRef] [Google Scholar] [Publisher Link]

[13] Xie Cheng, Sun Baigang, and Han Zhen, "Investigation on Jet Characteristics of Hydrogen Injection and Injection Strategy for Backfire Control in a Port Fuel Injection Hydrogen Engine," *Energy Procedia*, vol. 105, pp. 1588-1599, 2017. [CrossRef] [Google Scholar] [Publisher Link]

[14] Liqiang He et al., "The Impact from the Direct Injection and Multi-Port Fuel Injection Technologies for Gasoline Vehicles on Solid Particle Number and Black Carbon Emissions," *Applied Energy*, vol. 226, pp. 819-826, 2018. [CrossRef] [Google Scholar] [Publisher Link]

[15] Yonggyu Lee et al., "The Dual-Port Fuel Injection System for Fuel Economy Improvement in an Automotive Spark-Ignition Gasoline Engine," *Applied Thermal Engineering*, vol. 138, pp. 300-306, 2018. [CrossRef] [Google Scholar] [Publisher Link]

[16] Mohamed Ali Jemni et al., "Effects of Hydrogen Enrichment and Injection Location on in-Cylinder Flow Characteristics, Performance and Emissions of Gaseous LPG Engine," *Energy*, vol. 150, pp. 92-108, 2018. [CrossRef] [Google Scholar] [Publisher Link]

[17] Dengquan Feng et al., "Combustion Performance of Dual-Injection Using N-Butanol Direct-Injection and Gasoline Port Fuel-Injection in a SI Engine," *Energy*, vol. 160, pp. 573-581, 2018. [CrossRef] [Google Scholar] [Publisher Link]

[18] Seung Yeob Lee et al., "Effects of Injection Strategies on the Flow and Fuel Behavior Characteristics in Port Dual Injection Engine," *Energy*, vol. 165, pp. 666-676, 2018. [CrossRef] [Google Scholar] [Publisher Link]

[19] Jeongwoo Lee et al., "Comparison between Gasoline Direct Injection and Compressed Natural Gas Port Fuel Injection under Maximum Load Condition," *Energy*, vol. 197, 2020. [CrossRef] [Google Scholar] [Publisher Link]

[20] Farhad Salek et al., "Multi-Objective Optimization of the Engine Performance and Emissions for a Hydrogen/Gasoline Dual-fuel Engine Equipped with the Port Water Injection System," *International Journal of Hydrogen Energy*, vol. 46, no. 17, pp. 10535-10547, 2021. [CrossRef] [Google Scholar] [Publisher Link]

[21] Seonyeob Kim et al., "Effect of Boosting on a Performance and Emissions in a Port Fuel Injection Natural Gas Engine with Variable Intake and Exhaust Valve Timing," *Energy Reports*, vol. 7, pp. 4941-4950, 2021. [CrossRef] [Google Scholar] [Publisher Link]

[22] Helena Libalova et al., "Transcription Profiles in BEAS-2B Cells Exposed to Organic Extracts from Particulate Emissions Produced by a Port-Fuel Injection Vehicle, Fueled with Conventional Fossil Gasoline and Gasoline-Ethanol Blend," *Mutation Research/Genetic Toxicology and Environmental Mutagenesis*, vol. 872, pp. 1-12, 2021. [CrossRef] [Google Scholar] [Publisher Link]

[23] Jadi Raghu Varma et al., "Comprehensive Studies on Alcohol Using Port Fuel Injection Facilitated with Spark Plug Engine," *Materials Today: Proceedings*, vol. 45, no. 2, pp. 3219-3225, 2021. [CrossRef] [Google Scholar] [Publisher Link]

[24] Hayri Yaman, Murat Kadir Yesilyurt, and Samet Uslu, "Simultaneous Optimization of Multiple Engine Parameters of a 1-Heptanol / Gasoline Fuel Blends Operated a Port-Fuel Injection Spark-Ignition Engine Using Response Surface Methodology Approach," *Energy*, vol. 238, no. 3, 2022. [CrossRef] [Google Scholar] [Publisher Link]

[25] S. Molina et al., "Impact of Medium-Pressure Direct Injection in a Spark-Ignition Engine Fueled by Hydrogen," *Fuel*, vol. 360, pp. 1-12, 2024. [CrossRef] [Google Scholar] [Publisher Link]

[26] Fabian Musy et al., "Hydrogen-Fuelled Internal Combustion Engines: Direct Injection versus Port-Fuel Injection," *International Journal of Hydrogen Energy*, pp. 1-14, 2024. [CrossRef] [Google Scholar] [Publisher Link]